

Interpretation of the Gravity and Magnetic Anomalies of the Cappadocia Region, Central Turkey

A. BÜYÜKSARAC,¹ D. JORDANOVA,² A. ATEŞ,³ and V. KARLOUKOVSKI⁴

Abstract—The Cappadocia region, located in Central Turkey, is characterized by widespread lava flows and volcanoclastic deposits dating from Miocene to Quaternary. Gravity and aeromagnetic anomalies of the region appear to present similar high and low amplitude regions, although the aeromagnetic anomalies exhibit a rather complex pattern which is thought to be caused by remanent magnetization. The low-pass filtered aeromagnetic map shows a deep-seated magnetic anomaly which may be linked to the widespread volcanic activity at the surface. The pseudogravity transformation of the upward continued anomaly has been constructed. The pseudogravity anomaly demonstrates some form of clockwise rotation. This anomaly was modelled by means of a three-dimensional method. The top and bottom of the body are at 6.3km and 11km (including the flight height) from the ground surface, respectively. This deep body is ellipsoidal and extends along an E-W direction, which is in line with the regional stress direction deduced from GPS measurements. A new mobilistic dynamo-tectonic system appears to explain the body's E-W elongation. The modelled body may be the source for the inferred geothermal energy of the region. Magnetic measurements were carried out on oriented rock samples collected from outcrops of ignimbrites and basalts, providing directions and intensities of remanent magnetization, susceptibilities and Koeningsberger (Q) ratios. Standard deviations of remanent directions of the Natural Remanent Magnetization (NRM) display a wide scatter implying unreliability of the surface data. Reduction to pole (RTP) transformation of magnetic anomalies was successful with the induced magnetization angle despite the complex pattern of magnetic anomalies.

Key words: Magnetic and gravity anomalies, rock magnetic measurements, three-dimensional modelling, Cappadocia, Central Turkey.

Introduction

Cappadocia volcanic region is located between Aksaray, Nigde and Nevsehir towns, depicting a triangular shaped region in Central Anatolia. This region has been affected by major geologic and Alpine age events-products of recurrent relative movements between Africa and Eurasia. Cappadocia also exhibits complicated

¹ Department of Geophysical Engineering, Cumhuriyet University, Sivas, Turkey.
E-mail: absarac@cumhuriyet.edu.tr

² Geophysical Institute, Bulgarian Academy of Sciences, Acad. Bonchev Str., Block 3, 1113, Sofia, Bulgaria.

³ Department of Geophysical Engineering, Ankara University, Besevler, 06100, Ankara, Turkey.

⁴ Department of Geography, Lancaster University, Lancaster, LA14YB, United Kingdom.

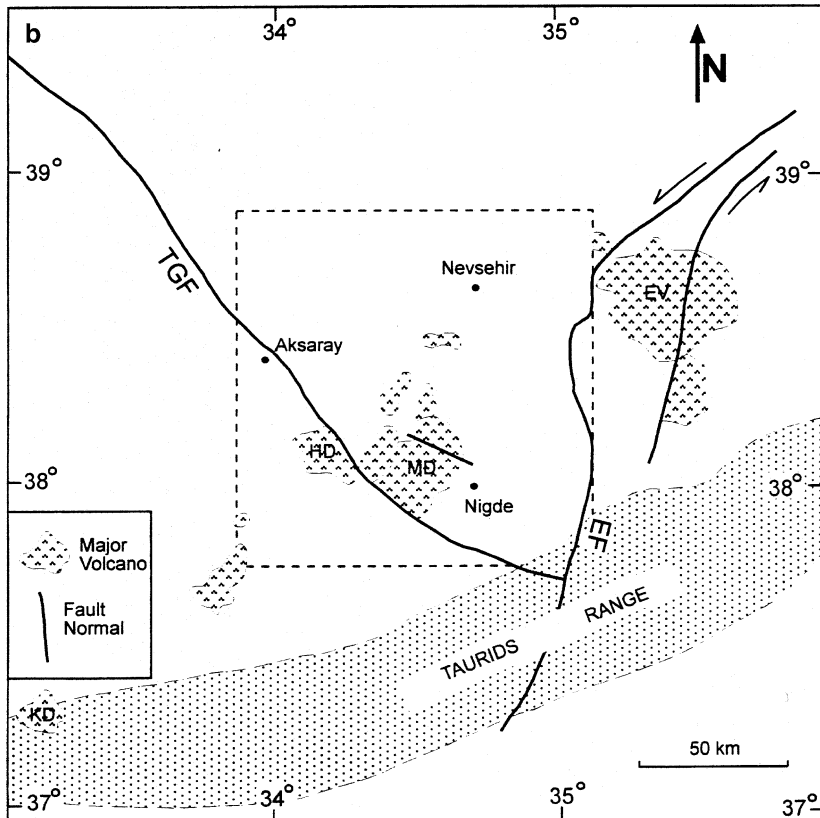
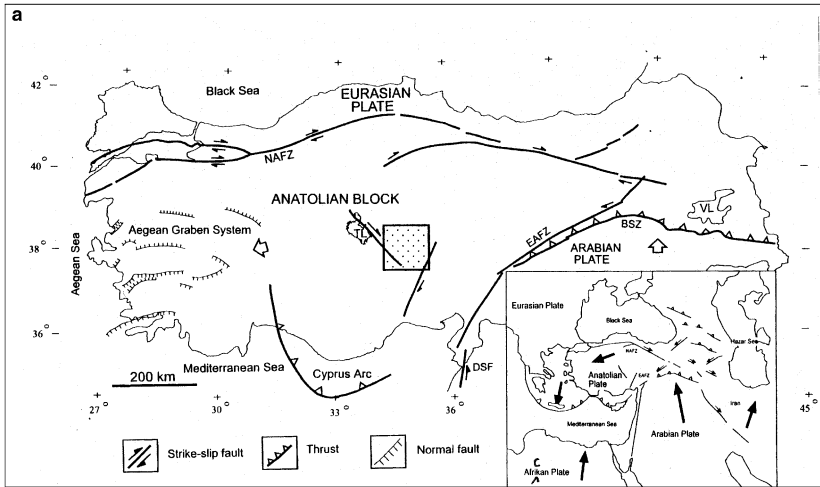
Figure 1

a) Simplified tectonic map of Turkey. The map was simplified from PIPER *et al.* (2002). Inset map shows the location and main tectonic units. NAFZ: North Anatolian Fault Zone, EAFZ: East Anatolian Fault Zone, BSZ: Bitlis Suture Zone, DSF: Dead Sea Fault, TL: Tuz Lake, VL: Van Lake. b) Simplified geological map of the study region. The map was simplified from DUHONT *et al.* (1998). The box with broken line shows the study area. TGF: Tuzgolu Fault, EF: Ecmis Fault, HD: Hasandagi Volcanites, MD: Melendizdagi Volcanites, KD: Kocdag Volcanites, EV: Erciyes Volcanites.

surface morphology related to recent volcanic activity. The basement consists of the metamorphic rocks of the Kirsehir Block, and tectonically the region is located at the junction of the active Tuz Lake and Ecmis faults. Simplified tectonic and geological maps of the region, based on PIPER *et al.* (2002) and DUHONT *et al.* (1998), are given in Figures 1a and b. A number of geological and geophysical surveys has recently been carried out in specific areas. TOPRAK (1998) investigated surface features using geological methods and ILKISIK *et al.* (1997) studied the geothermal field potential of the Ihlara Valley, east of Cappadocia, using geoelectromagnetic and geothermic methods from which they suggested a modest geothermal potential and the presence of some undiscovered fields. FROGER *et al.* (1998) explored the hidden calderas by using multi-source geophysical data. Available palaeomagnetic data for central Anatolia were summarized by PIPER *et al.* (2002) who suggested anticlockwise rotation of the Cappadocia volcanic complex and clockwise rotation in the western extremity of the Anatolian collage. Aeromagnetic survey of Turkey reveals circular-shaped anomalies over the Cappadocia region centered on (38°15'N; 34°30'E) (ATES *et al.*, 1999). The Curie point depth map of Central Anatolia, estimated from aeromagnetic anomalies, demonstrates shallow Curie depth over Cappadocia and Erciyes volcanic regions (ATES *et al.*, 2005). In this paper, the deep structure of the study area is investigated by means of processing and interpreting aeromagnetic and gravity anomalies. A deep-seated magnetic anomaly was modelled by a three-dimensional method. The thickness of this body is calculated to be approximately 4 km with its top at 5.7 km below the ground surface. This deep magnetic body appears to be the source of the widespread volcanic activity at the surface. The body has an ellipsoidal shape extending approximately in an E-W direction which is in line with the regional present-day shear stress direction obtained from GPS measurements (MCCLUSKY *et al.*, 2000). Aeromagnetic anomalies were also correlated with magnetic measurements carried out on rock samples collected from the region.

Aeromagnetic and Gravity Data

Aeromagnetic and gravity surveys of entire Turkey were carried out by the General Directorate of the Mineral Research and Exploration of Turkey (MTA) (ATES *et al.*, 1999). In central Turkey, the gravity data were collected at 1–3 km intervals; all necessary corrections to the raw gravity measurements being carried out



by the MTA. Gravity anomalies of the Cappadocia region are shown in Figure 2. The aeromagnetic data were taken with 1–2 km profile intervals and with approximately 70 m sampling from 600 m above the ground surface. All necessary corrections related to the survey data were done by the MTA, except for the International Geomagnetic Reference Field (IGRF) corrections which were carried out by the present authors applying the algorithm of BALDWIN and LANGEL (1993). The corrected residual total magnetic intensity anomalies are shown in Figure 3. Most of the magnetic anomalies are disoriented from the magnetic N-S, direction suggesting the effect of remanent magnetization. Both data sets were gridded by the MTA, employing a standard interval of 2.5 km. From the resulting gravity map, two relatively well-defined anomalies can be discerned: A gravity high to the north and a gravity low to the south. The two gravity anomalies are superposed on the

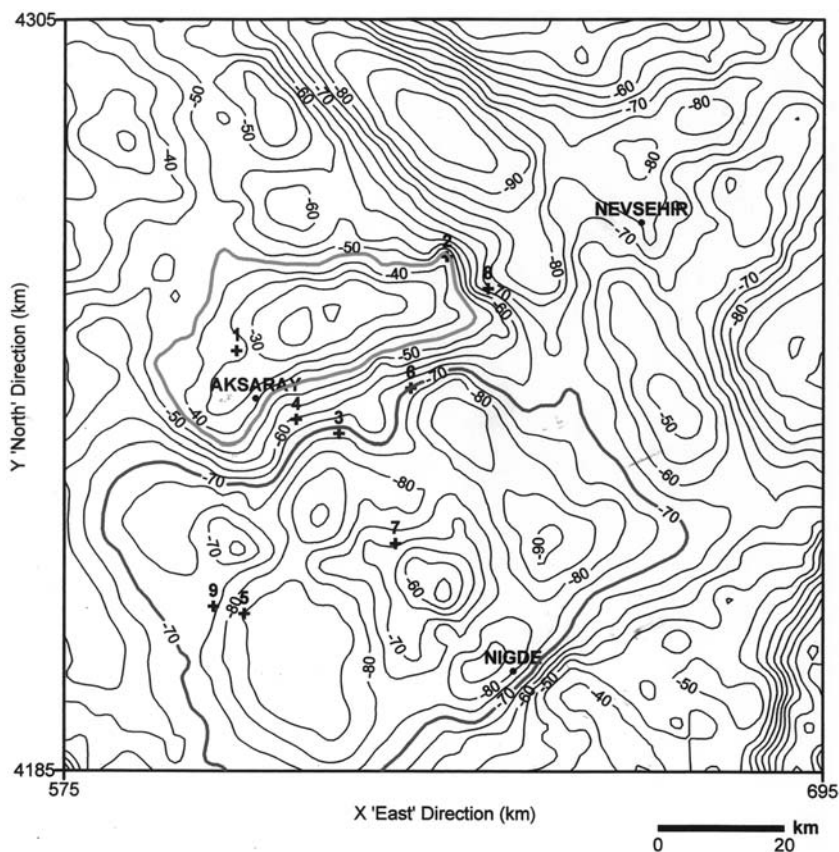


Figure 2

Gravity anomaly map of the region. Contour interval is 5 mGal. Gravity high and low amplitude regions are annotated with red and blue lines, respectively. Numbers from 1 to 9 with + signs show the sampling locations.

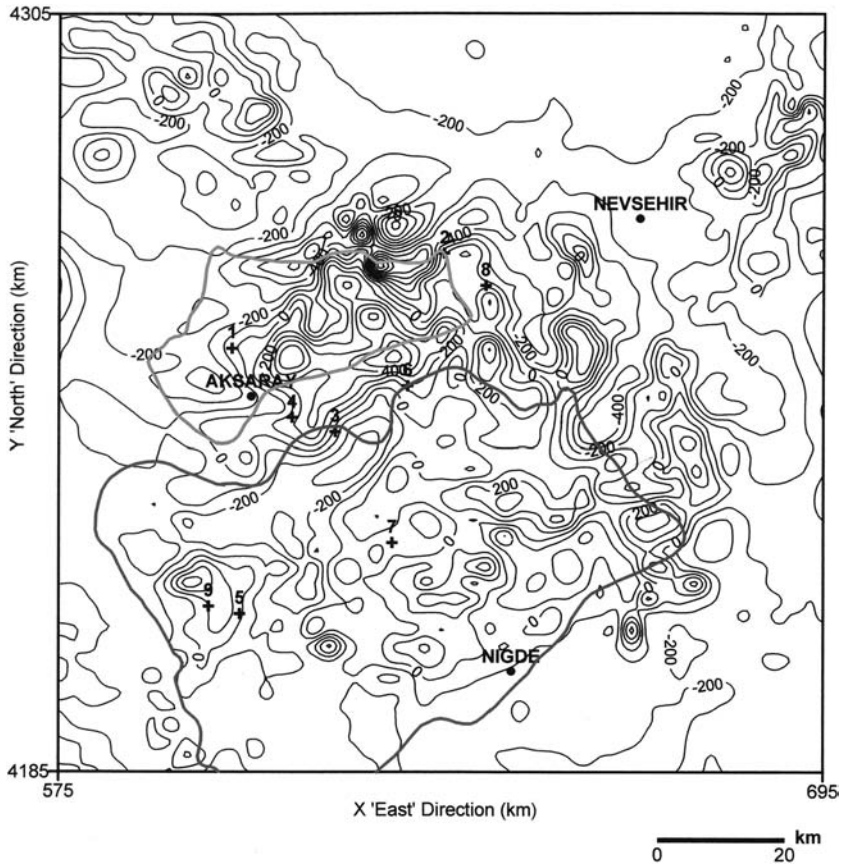


Figure 3

The residual total magnetic intensity anomaly map. Contour interval is 100 nT. Gravity high and low amplitude regions are annotated with red and blue lines, respectively. Numbers from 1 to 9 with + signs show the sampling locations.

aeromagnetic anomaly map of Figure 3. As can be seen from the latter diagram, the gravity anomalies are in close correspondence with the more rugged magnetic anomaly picture.

Power Spectrum Analysis of Aeromagnetic Anomalies

The power spectrum of the gridded aeromagnetic data set described above was computed using the method of SPECTOR and GRANT (1970). Figure 4 shows graphs of the logarithm of azimuthally averaged power spectrum against wavenumber ($K/2\pi$). A mean depth (z) of the anomaly source may be obtained by fitting linear segments to the power spectrum graphs by utilizing the equation

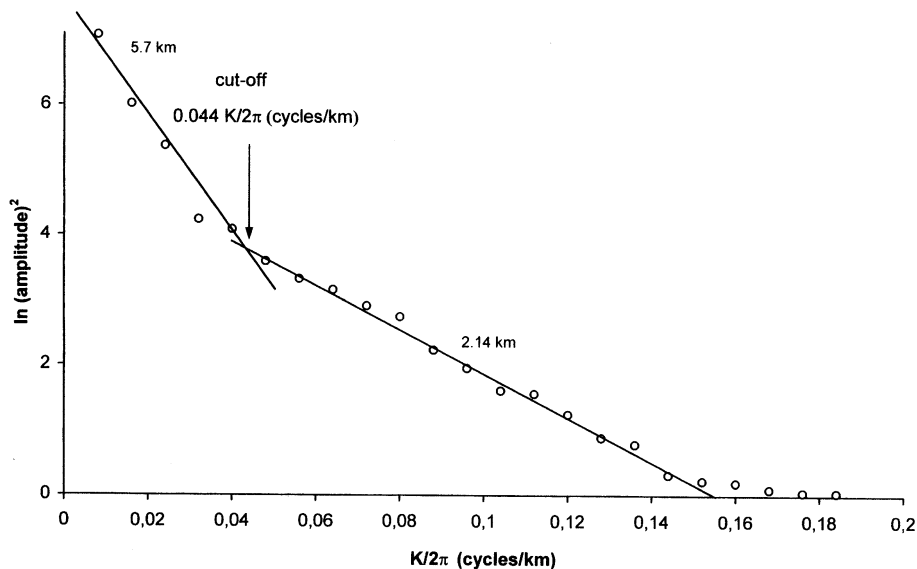


Figure 4

Power spectrum graphic. Logarithmic power versus wavenumber ($K/2\pi$).

$z = -(\Delta \log_e P / \Delta k) / 4\pi$ from SPECTOR and GRANT (1970). The two linear segments in Figure 4 correspond to source depths of 6.3 and 2.74 km (including the flight height), respectively.

Filtering and Upward Continuation

To enhance the effect of the deep source aeromagnetic anomalies shown in Figure 3, low-pass filtering using the cut-off frequency was obtained from the wavenumber of the crossing segments of the shallow and deep sources (Fig. 4). The cut-off frequency obtained in this manner is $0.044 K/2\pi$. The low-pass filtered map (Fig. 5) cannot easily be interpreted as no information can be derived regarding the depth extent of the source. This was probably caused by overlapping high and low frequencies. Upward continuation is an analogous form of low-pass filtering and can be done by multiplying the Fourier transform of the anomaly by $\exp\left[-2\pi h(k_x^2 + k_y^2)^{1/2} / N\right]$ (KANASEWICH and AGARWAL, 1970), where h is the continuation distance, k_x and k_y are the wavenumbers in the x and y spatial directions and N is the total number of data points (grid numbers). A 14 km (including 0.6 km flight height) upward continued magnetic field is shown in Figure 6. Upward

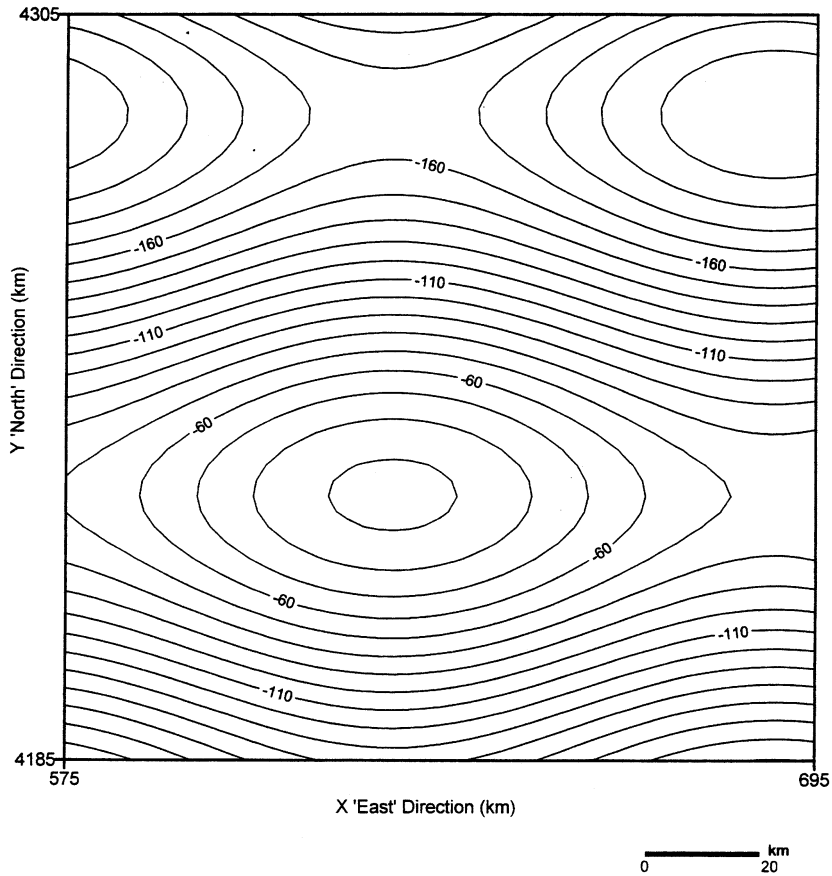


Figure 5
Low-pass filtered aeromagnetic anomaly map. Contour interval is 10 nT.

continued aeromagnetic anomalies produce a field similar in shape and amplitude to the low-pass filtered anomaly.

Interpretation of the Deep-seated Magnetic Body

It is possible to interpret the upward continued magnetic field by three-dimensional methods. In this work, interpretation of the pseudogravity transformation of the upward continued field was chosen. It is easier to constrain the pseudogravity field as the distortion caused by the total magnetization vector is removed (KEAREY and BROOKS, 1991). Figure 7 shows the pseudogravity transformed field computed for induced magnetization (declination angle 4° , inclination

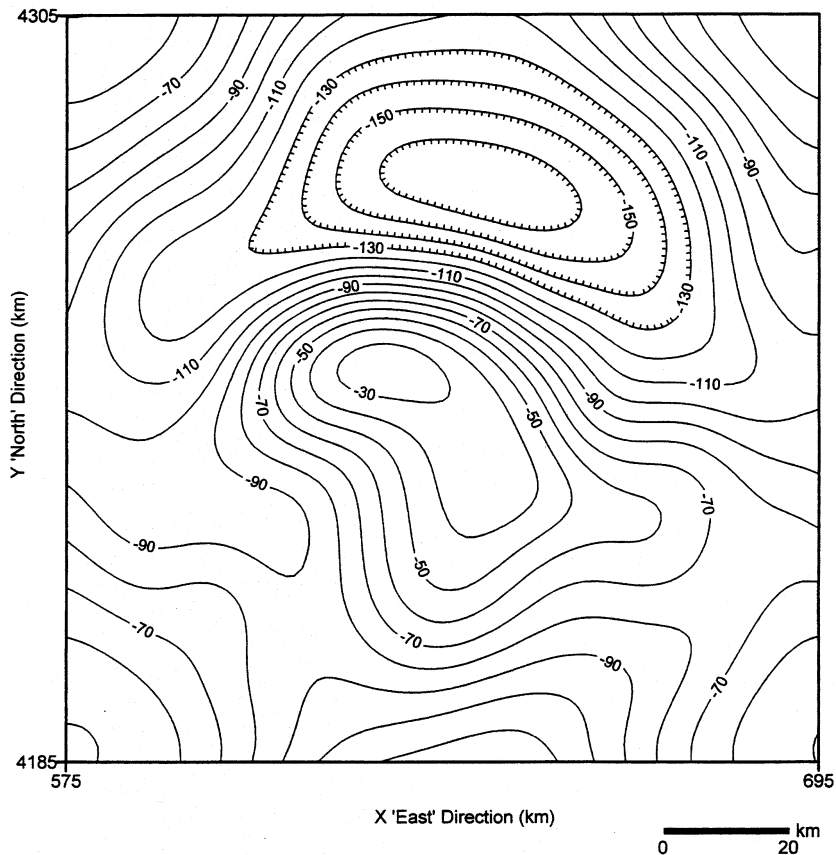


Figure 6

Upward continuation anomaly map. Continuation height is 14 km (including 0.6 km flight height). Contour interval is 10 nT.

angle 55°N) and body magnetization (declination angle 30° , inclination angle 55°N) utilizing the algorithm of BLAKELY (1995). 30° of declination angle of the body magnetization is deduced from the orientation of the positive and negative peaks of anomaly field of the upward continued map. This method of determining magnetization may be in error, as the causative body is assumed to have uniform magnetisation and this may not be the case.

Three-dimensional Magnetic Modelling

A three-dimensional model of the pseudogravity anomaly (Fig. 7) was constructed by using the algorithm of CORDELL and HENDERSON (1968). This method is based on simulating the gravity anomalies of a group of vertical rectangular prisms

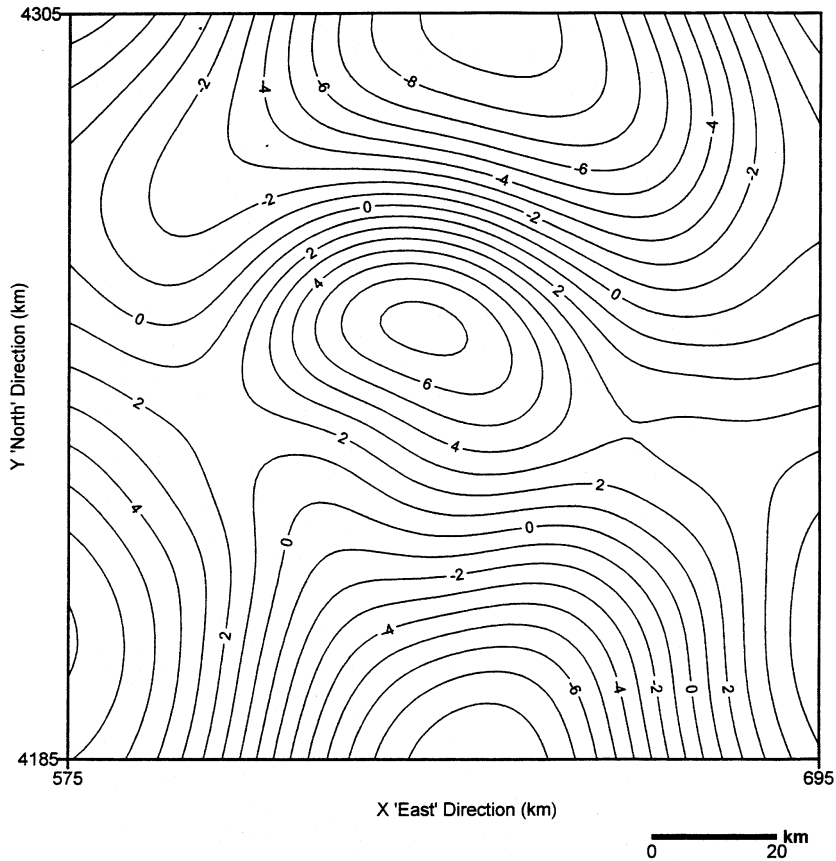


Figure 7

Pseudogravity anomaly map of Cappadocia. Contour interval is 1 mGal, Inclination and declination angle of the induced magnetization are 55° and 4° , respectively. Inclination and declination of the body magnetization are 55° and 30° , respectively.

to the observed field of which is the pseudogravity data in this case. This method of modelling can be achieved by choosing either a common base, top or centre. Altogether 1936 prisms with 2.5×2.5 km dimension in X and Y directions were chosen to have a common base. The bottom depth of the model was changed until the top of the model reached 5.7 km depth from the surface as determined by the power spectrum analysis. In this case, the base of the model remained at 11 km from the surface (Fig. 8). The shape of the body resembles an ellipsoid elongated almost in E-W direction. The base of the model at 11 km also agrees well with the information derived from the Curie point depth map of central Anatolia (ATES *et al.*, 2005). A three-dimensional model was constructed similarly by KEAREY (1991) who suggested

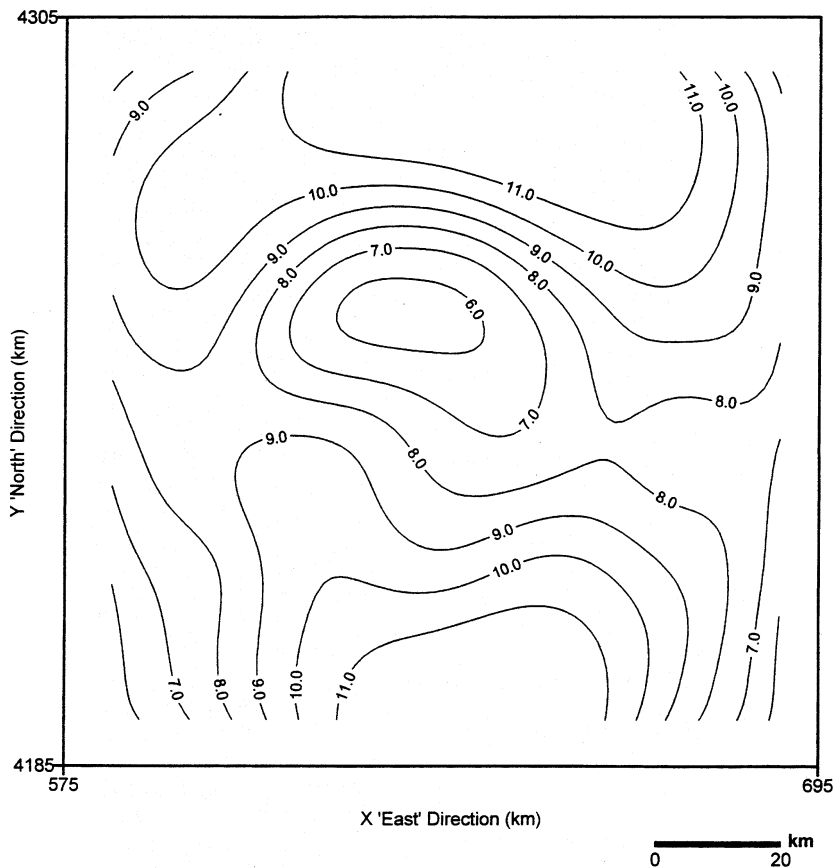


Figure 8

Three-dimensional model of the pseudogravity anomaly map of Figure 7. Contour interval is 1 km.

a possible basaltic source beneath the London Platform, south-central England. Deep structures of the Mendip Hills and Worcester graben, southern England, were similarly constructed by three-dimensional modelling by ATES and KEAREY (1993) and ATES and KEAREY (1995), respectively.

Interpretation of the Shallow Magnetic Body

To enhance the effect of the shallow sources, high-pass filtered aeromagnetic anomalies were produced using the aforementioned cut-off frequency. In Figure 9, peak to trough axes of the anomalies are marked with red arrows to demonstrate disorientation from the magnetic N-S direction. Reduction to pole transformation

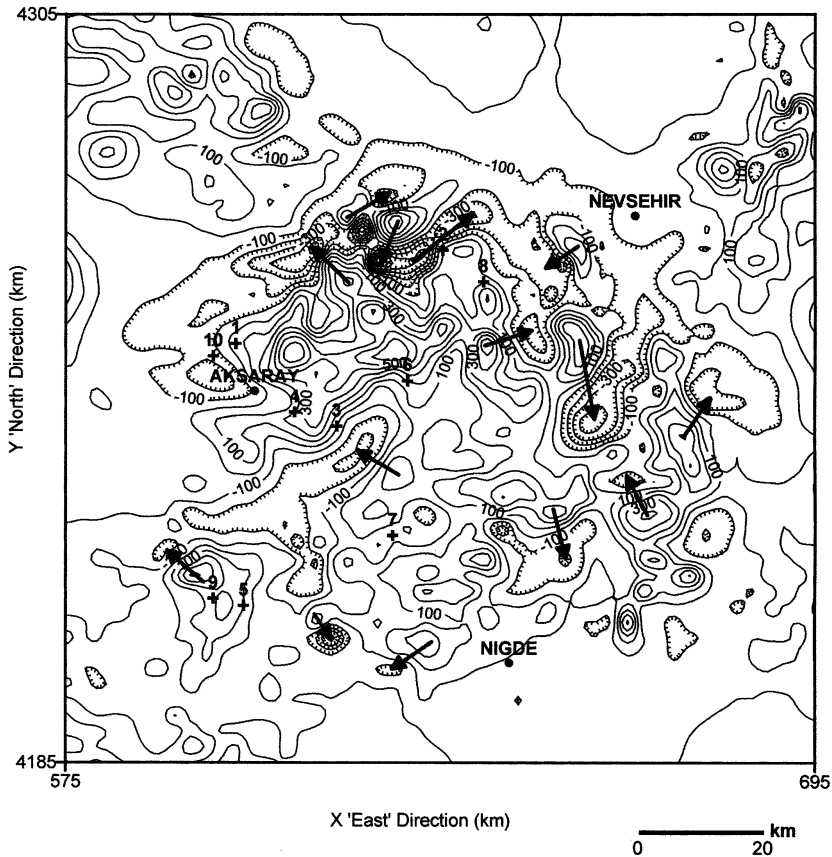


Figure 9

High-pass filtered aeromagnetic map. Peak to trough axes are indicated by red arrows. Contour interval is 100 nT. Numbers from 1 to 9 with + signs show the sampling locations. Lows are hachured.

(RTP), which removes the distortion caused by the Earth's magnetic field, was applied to the residual aeromagnetic anomalies using the magnetization angle of the induced magnetization. RTP transformation was successful; disoriented anomalies were removed and no polarities can be observed. Thus, it may be suggested that the remanent components of the magnetization appear to be self-erasing. The RTP transformed map is shown in Figure 10.

Magnetic Properties of Surface Formations

Several formations of Cappadocia ignimbrites and basaltic andesites have been sampled at 12 locations with coordinates varying between 34–35°E and 37.45–38.50°N. The corresponding axial dipole field has a declination of 4° and an

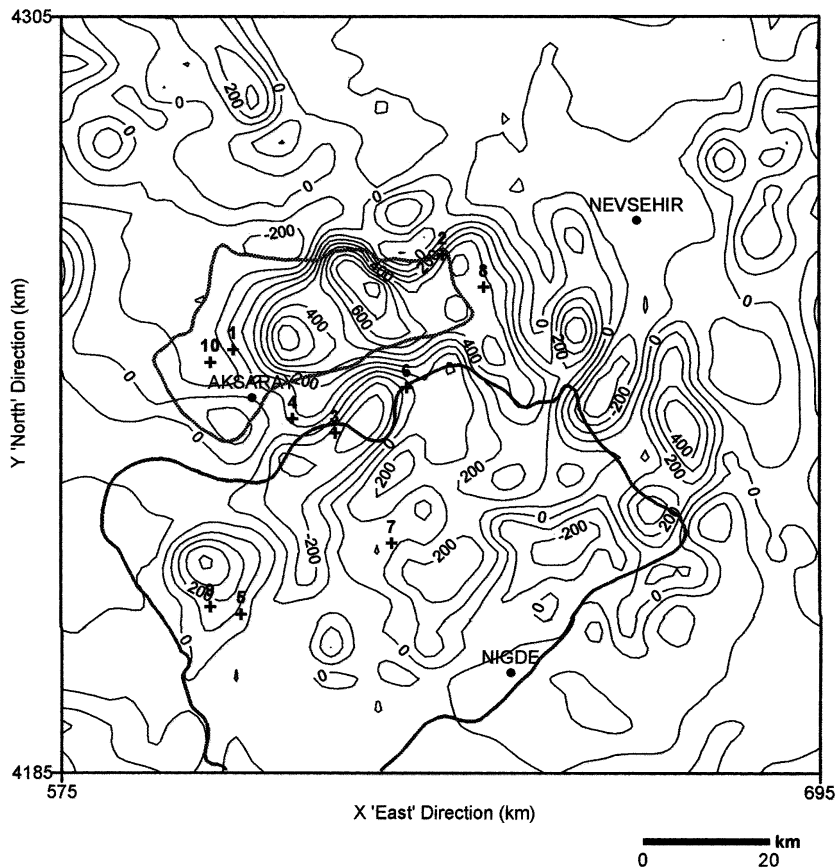


Figure 10

Reduction to pole transformation (RTP) of aeromagnetic anomalies. Contour interval is 100 nT. Gravity high and low amplitude regions are annotated with red and blue lines, respectively.

inclination of 55° . Sixty-eight oriented hand samples have been gathered using magnetic and sun compasses. From each sample, 3–7 cubic specimens were cut in the laboratory. This resulted in a collection of 270 specimens. Measurements of the Natural Remanent Magnetization (NRM) and their average inclination and declination angles (I_{mean} and D_{mean}), low-field magnetic susceptibility (K) were carried out for the various rock formations. Such information may in some cases be important for interpreting magnetic anomaly maps. For the same purpose, calculations of Koeningsberger ratio $Q = \text{NRM}/hK$ (h — intensity of the present magnetic field, K — low-field magnetic susceptibility) were performed on all the specimens.

The wide range of Q -ratios points significant contributions of both induced and remanent magnetization components to the anomaly map. On the other hand,

Gelveri (GL) and Kizilkaya (KZ) formations were sampled in two different locations, however the distributions of NRM and K values show insignificant differences. Significant magnetic inhomogeneities within the ignimbritic bodies may be an additional factor for anomaly distortion. This is especially important as KZ is the youngest unit of the succession and more highly contributes to the surface anomalies. The rhyolitic ignimbrites from Acigol (AG) are characterized by three orders of magnitude lower values of NRM and K (Table 1), nonetheless relatively high Q -ratios suggest the importance of remanent magnetization (Table 1).

Andesitic basalts sampled at Kiziltepe (KT) are highly magnetic rock formations, with NRM intensities of 60 Am^{-1} and susceptibilities of $21 \times 10^{-3} \text{ SI}$ (Table 1). At the same time, Q -ratios are extremely high (Table 1), pointing to a major role of remanence in the total magnetic anomalies. Similarly, Hasandagi (H) and Kecikalesi (KK) basaltic andesites show relatively high NRM intensities, high susceptibilities and high Q -ratios (Table 1). Andesites displaying high amplitude anomalies were sampled at Melendizdag (MZ) and Erdas (ER); these rocks are characterized by relatively low NRM intensities and relatively high susceptibilities, resulting in low Q -ratios (Table 1).

Conclusions

The aeromagnetic map of Cappadocia (Fig. 3) exhibits complicated anomaly patterns. In the northern sector there are stronger magnetic field anomalies than in the southern sector. In both areas the magnetic anomaly picture is found to correlate with corresponding gravity anomalies (Fig. 3).

Upward continued aeromagnetic anomalies (Fig. 6) clearly demonstrate that the deep magnetic body must have a magnetization vector in a different orientation from that of the present Magnetic Field (declination 4°E , inclination 55°). Therefore, remanent magnetization component must be present. In this case, a 30° of declination of total magnetization can be observed, suggesting a clockwise rotation of the deep-seated magnetic body. Adding to the tectonic complexity of the region, clockwise rotation of the western extremity of the Cappadocian collage has been suggested by palaeomagnetism (PIPER *et al.*, 2002).

STORETVEDT *et al.* (1999), based on a palaeomagnetic study of alkaline igneous rocks of the French Pyrenees concluded that during the Alpine climax the Iberian Peninsula first rotated 40° counterclockwise and then 70° clockwise. The reason for this rotational instability is that the Peninsula is located within the tectonically strained Alpine region, being squeezed in between the oppositely rotating Eurasia and Africa megablocks.

STORETVEDT (2003) described a new tectonic model suggesting complex rotational behavior of micro-blocks within the overall transpressive Alpine fold

Table 1

Median values of NRM intensities, magnetic susceptibilities and Q-factors for the formations studied. IG: İğnimbrites, AG: Açıgöl, IG_{GL}: Gelveri ignimbrites, IG_{KZ}: Kizilkaya ignimbrites, H: Hasandagi, KT: Kızıltepe, MZ: Melendizdagi, ER: Erdas, KK: Keciakesi. Parentheses in site numbers show sampling localities in Figures 2, 3, 9 and 10. Numbers in parentheses with I_{mean} and D_{mean} angles show standard deviations

Rock type	Site	Coordinate	Number of Samples	NRM intensity (mA/m)	Dmean	Imean	K ($\times 10^3$ SI)	Q-ratio	Density (gr/cm ³)
İğnimbrites	(1) IG	38°24.66 N 34°10.20 E	53	546	174.36 (70.02)	-16.38 (38.35)	5.338	2.5	1.8
	(2) AG	38°32.52 N 34°33.17 E	33	172	198.07 (111.87)	67.39 (15.79)	0.153	11.7	1.9
	(3) IG _{GL}	38°17.40 N 34°21.18 E	17	2177	165.82 (33.69)	-18.87 (35.6)	6.7	6.16	2.0
Andesites + Basalts	(4) IG _{KZ}	38°18.66 N 34°16.58 E	14	1061	164.79 (50.34)	-5.45 (14.89)	5.164	5.14	1.8
	(5) H	38°01.95 N 34°10.71 E	29	7452	179.58 (142.59)	45.13 (25.37)	12.447	18.8	2.7
	(6) KT	38°21.20 N 34°29.06 E	34	59080	183.65 (123.42)	-0.25 (32.58)	21.2	74.5	2.9
	(7) MZ	38°07.84 N 34°27.16 E	28	293	189.76 (90.99)	-46.04 (27.60)	9.108	0.78	2.8
	(8) ER	38°27.70 N 34°37.62 E	29	812	139.19 (65.47)	-36.25 (22.97)	20.113	0.97	2.9
	(9) KK	38°02.62 N 34°07.38 E	24	2308	232.33 (90.89)	15.52 (37.15)	13.784	4.6	2.8

belt. The opposite rotations of Africa and Eurasia were caused by a global inertia effect, although the resulting shearing along the Africa-Europe tectonic boundary could also produce smaller scale transtensions. Owing to its location within the complex Alpine Belt, the Cappadocia region is most likely to have been a strained area throughout Alpine time. Thus, several authors have arrived at anticlockwise rotation for Anatolia.

In a recent publication, McCLUSKY *et al.* (2000) described the anticlockwise rotation of Anatolia from GPS measurement, in association with a westward movement of this block when viewed in a Eurasia-fixed frame. The approximately E-W elongated deep-seated magnetized body of the present study (Fig. 8) is likely to be produced by the overall E-W oriented shear stress as depicted from GPS measurements. The bottom depth of this magnetic body is at 11 km from surface, corresponding to the Curie Point Depth of central Anatolia estimated by ATES *et al.* (2005). This deep-seated magnetized body may be the source for the widespread volcanic activity of the Cappadocia region.

In a northern hemisphere location the characteristic magnetic anomalies of a dipolar source can have a positive peak in the south and a smaller negative peak in the north, but remanent magnetization with a different direction to that of the Earth's induced magnetic field, with high Q -ratio (Table 1), can affect the shape and orientation of the magnetic anomalies. Such distortions can be seen from the observed residual and high-pass filtered aeromagnetic anomalies of Cappadocia (Figs. 3 and 9). Shape analysis suggests that most of the anomalies have a total magnetization direction differing from the induced one. Anomalies with 'anomalous' shape are indicated with red arrows in the high-pass filtered anomalies (Fig. 9) with the arrow pointing in peak to trough direction. Anomalies with similar characteristics have been reported from the Italian region by FEDI *et al.* (1991; 1999). The latter authors suggested dominant effects from remanent magnetization and that the regions investigated had experienced rotations in different directions.

Samples collected at outcrop numbers 1 to 4 are from ignimbrites; their locations are to the northwest of the Cappadocia region where high amplitude magnetic anomalies are found (Fig. 3). Ignimbrites have a maximum susceptibility (K) of 6.7×10^{-3} SI at location 3 (Gelveri) which would produce 0.3 Am^{-1} in intensity of induced magnetization (the absolute K values are corrected for the real volume of the samples in respect to the nominal volume for the Kappabridge KLY-2, used for susceptibility measurements). This intensity of magnetization would not be strong enough to produce the required amplitude of the magnetic anomalies in this region. Densities of ignimbrites are in the range of $1.8\text{--}2.0 \text{ gr/cm}^3$ (Table 1) in the region where high intensity of gravity anomalies occurs (Fig. 2), low to produce the high, i.e. too amplitude gravity anomaly. Magnetic bodies, expressing higher intensity of magnetization than the formations at surface, must be present at depth.

Andesitic basalts were collected from outcrop numbers 5 to 9 (Fig. 3), located to the southeast of the ignimbrites. Magnetization measurements indicate maximum

susceptibility (K) of 21.2×10^{-3} SI at Kiziltepe (KT) (locality no: 6), giving rise to an induced intensity of magnetization of 0.967 Am^{-1} . However, the measured remanent magnetization at this location is 59.08 Am^{-1} , and magnetic substances with such NRM intensity would produce much stronger magnetic anomalies. The observed complex pattern of magnetic anomalies with high NRM intensities could be produced by an association of smaller scale anticlockwise and clockwise rotations. RTP transformed anomalies (Fig. 10) show an undisturbed pattern of magnetic anomalies and thus remanent components appear to be self-cancelling. High value of standard deviations in I_{mean} and D_{mean} values support this suggestion (Table 1). The complex picture of surface rotations, deduced from high-pass filtered magnetic anomalies (Fig. 9), does not match the magnetization direction of the deep-seated magnetic anomaly (Fig. 6) which apparently has been dominantly affected by the longstanding counter clockwise rotation of Africa.

Acknowledgements

The authors wish to thank Dr. K. M. Støretvedt of the University of Bergen for his critical review of the manuscript and many helpful comments suggested. We extend our thanks Talat Yildirim of the General Directorate of Mineral Research and Exploration of Turkey (MTA) for his aid during sample collection and his informative discussions on the geology of the Cappadocia Region. Funda Bilim helped with the RTP calculation. Our appreciation is to MTA for the provision of aeromagnetic and gravity data. A. Büyüksaraç and A. Ateş are grateful to the Geophysical Institute of the Bulgarian Academy of Sciences (BAS) for the invitation to carry out magnetic work in the Palaeomagnetic Laboratory in Sofia. This research was financially supported by the Ankara University, Directorate of Research Fund (Project code: 20010705050).

REFERENCES

- ATES, A., BILIM, F., and BÜYÜKSARAC, A. (2005), *Curie Point Depth Investigation of Central Anatolia, Turkey*, Pure Appl. Geophys., 162, 357–371
- ATES, A. and KEAREY, P. (1993), *Deep Structure of the East Mendip Hills from Gravity, Aeromagnetic and Seismic Reflection Data*, J. Geol. Soc., London, 150, 1055–1063.
- ATES, A. and KEAREY, P. (1995), *A New Method for Determining Magnetization Direction from Gravity and Magnetic Anomalies: Application to the Deep Structure of the Worcester Graben*, J. Geol. Soc. London, 152, 561–566.
- ATES, A., KEAREY, P. and TUFAN, S. (1999), *New Gravity and Magnetic Maps of Turkey*, Geophys. J. Int. 136, 499–502.
- BALDWIN, R.T. and LANGEL, R. (1993), *Tables and Maps of the DGRF 1985 and IGRF 1990*. International Union of Geodesy and Geophysics Association of Geomagnetism and Aeronomy, IAGA Bulletin No. 54, 158 pp.
- BLAKELY, R.J., *Potential Theory in Gravity and Magnetic Applications* (Cambridge University Press, 1995) 441 pp.

- CORDELL, L. and HENDERSON, R.G. (1968), *Iterative Three-dimensional Solution of Gravity Anomaly Data Using a Digital Computer*, *Geophys.* 33, 596–601.
- DUHONT, D., CHOROWICZ, J., YURUR, T., FROGER, J.L., KOSE, O., and GUNDOGDU, N. (1998), *Emplacement of Volcanic Vents and Geodynamics of Central Anatolia, Turkey*, *J. Vol. Geothermal Res.* 85, 33–54.
- FEDI, M., FLORIO, G., and RAPOLLA, A. (1991), *The Role of Remanent Magnetization in the Southern Italian Crust from Aeromagnetic Anomalies*, *Terra Nova* 2, 629–637.
- FEDI, M., FLORIO, G., and RAPOLLA, A. (1996), *Palaeomagnetism and Tectonics of the Mediterranean Region* (eds. Morris, A. and Tarling, D. H.), *J. Geol. Soc. London, Spec. Publ.* 105, 147–152.
- FROGER, J.L., LENAT, J.F., CHROWICZ, J., LE PENNEC, J.L., BOURDIER, J.L., KOSE, O., ZIMITOGLU, O., GÜNDOGDU, N.M., and GOURGAUD, A. (1998), *Hidden Calderas Evidenced by Multisource Geophysical Data; Example of Cappadocian Calderas, Central Anatolia*, *J. Vol. Geothermal Res.* 185, 99–128.
- ILKISIK, M., GÜRER, A., TOKGÖZ, T., and KAYA, C. (1997), *Geoelectromagnetic and Geothermic Investigations in the Ihlara Valley Geothermal Field*, *J. Vol. Geothermal Res.* 78, 297–308.
- KANASEWICH, E.R. and AGARWAL, R.G. (1970), *Analysis of Combined Gravity and Magnetic Fields in Wavenumber Domain*, *J. Geophys. Res.* 75, 5702–5712.
- KEAREY, P. (1991), *A Possible Source of the South-central England Magnetic Anomaly: Basaltic Rocks beneath the London Platform*, *J. Geol. Soc. London* 148, 775–780.
- KEAREY, P. and BROOKS, M., *An Introduction to Geophysical Exploration*, Second edition (Blackwell Scientific Publications, Oxford 1991) pp. 250.
- MCCLUSKY, S., BALASSANIAN, S., BARKA, A., DEMIR, C., ERGINTAV, S., GEORGIEV, I., GURKAN, O., HAMBURGER, M., HURST, K., KAHLE, H., KASTENS, K., KEKELIDZE, G., KING, R., KOTZEV, V., LENK, O., MAHMOUD, S., MISHIN, A., NADARIYA, M., OUZOUNIS, A., PARADISSIS, D., PETER, Y., PRILELIN, M., REILINGER, R., SANLI, I., SEEGER, H., TEABLEB, A., TOKSÖZ, M.N., and VEIS, G. (2000), *Global Positioning System Constraints on Plate Kinematics and Dynamics in the Eastern Mediterranean and Caucasus*, *J. Geophys. Res.* 105, 5695–5719.
- PIPER, J.D.A., GURSOY, H., and TATAR, O. (2002), *Palaeomagnetism and Magnetic Properties of the Cappadocian Ignimbrite Succession, Central Turkey and Neogene Tectonics of the Anatolian Collage*, *J. Vol. Geothermal Res.* 117, 237–262.
- SPECTOR, A. and GRANT, F.S. (1970), *Statistical Models for Interpreting Aeromagnetic Data*, *Geophys.* 35, 293–302.
- STORETVEDT, K. M., *Global Wrench Tectonics* (Fagbokforlaget, Norway, 2003) pp.397.
- STORETVEDT, K. M., MARTON, E., ABRANCHES, M.C., and ROTHER, K. (1999), *Alpine Remagnetisation and Tectonic Rotations in the French Pyrenees*, *Geol. Rundsch.* 87, 658–674.
- TOPRAK, V. (1998), *Vent Distribution and its Relation to Regional Tectonics, Cappadocian Volcanics, Turkey*, *J. Vol. Geothermal Res.* 85, 55–67.

(Received November 10, 2003; accepted August 11, 2004)

Published Online First: July 29, 2005



To access this journal online:

<http://www.birkhauser.ch>
